Journal of Applied Mechanics Vol.11, pp.1015-1022 (August 2008) JSCE

Dynamic response evaluations of dual cylindrical structure due to wave force

Min-su Park * and Kenji Kawano **

* Graduate Student, Dept. of Ocean Civil Eng. Kagoshima University (1-21-40, Korimoto, Kagoshimasi 890-0065)
** Member Dr. of Eng., Prof. Dept. of Ocean Civil Eng. Kagoshima University (1-21-40, Korimoto, Kagoshimasi 890-0065)

Great possibilities to develop ocean spaces which may be used as resident areas, airports, power stations, etc. could be provided by offshore structure with a large deck area. In the present study, it is examined about the dynamic response characteristics on a dual cylindrical structure consisting of a thin and porous outer cylinder with an impermeable inner cylinder. The evaluation of the wave force on the dual cylindrical structure, under the assumption of potential flow and linear wave theory, is carried out with an eigenfunction expansion method. It is shown that the outside cylinder with porosity plays important roles on the reduction of dynamic responses of the dual cylindrical structure for the severe wave condition.

Key Words: *diffraction theory, eigenfuntion expansion method, dual cylindrical structure, dynamic response.*

1. Introduction

Since the wave force is one of the most important forces on an offshore structure, the dynamic response evaluation due to wave forces has significant roles on the reliable design of the offshore structure. The wave forces on an offshore structure can be usually obtained by diffraction theory. The wave diffraction problem about a vertical circular cylinder can be solved with analytical solution in ocean engineering(MacCamy & Fuchs (1954)). When a wave is incident on a group of cylinders, it is necessary to consider not only the diffraction due to each cylinder but also the multiple scattering due to the presence of neighboring cylinders with the group. Under the assumptions of potential flow and linear wave theory, a semi-analytical solution for impermeable cylinders has been obtained by an eigenfunction expansion approach proposed by Spring & Monkmeyer (1974), and simplified by Linton & Evans(1990) for N bottom-mounted circular cylinders. It has been examined about the cylindrical structure which the outer cylinder is porous and considered to be thin in thickness and the inner cylinder is impermeable(Wang & Ren(1994), Sankarbabu, et al(2007)). It is indicated that the hydrodynamic force on the inner cylinder can be effectively reduced by the existence of outer porous cylinder. It is supposed that it is important to clarify the dynamic response characteristics for developing the dual cylindrical structure.

In the present study, the eigenfunction method is applied to evaluate the wave force on arrayed dual cylindrical structures which consist of an impermeable inner cylinder and a porous outer cylinder. The present numerical method is compared with the results from Wang & Ren(1994). The wave force and wave run up on the inner and outer cylinder with the interaction to regular waves are examined in cases the number of dual cylindrical structure is single and four. Applying the wave force evaluated by the present method, the dynamic response of the dual cylindrical structure is carried out with the modal analysis that can be solved by step-by-step integration such as Newmark β method(Kawano, et al.(1990)). It is examined about the dynamic response characteristics due to wave forces affected by the porosity of outer cylinder. It is shown that the dynamic response of the dual cylindrical structure can be effectively reduced by the outside cylinder with appropriate porosity.

2. Formulation

2.1 Wave force interaction on dual cylindrical structure

It is assumed that the fluid is inviscid, and incompressible, and its motion is irrotational. An arbitrary array of N bottom-mounted dual circular cylinders is situated in water of uniform depth h. The radius of the jth outer cylinder is a_j and that of the corresponding inner cylinder is b_j. The global Cartesian coordinate system(x, y, z) is defined with an origin located on the still-water level with the z-axis directed vertically upwards. The center of each cylinder at (x_j, y_j) is taken as the origin of a local polar coordinate system (r_j, θ_j), where θ_j is measured counterclockwise from the positive x-axis. The center of the kth cylinder has polar coordinates (R_{jk}, α_{jk}) relative to the jth cylinder. The coordinate relationship between the jth and kth cylinders is shown in Fig. 1.

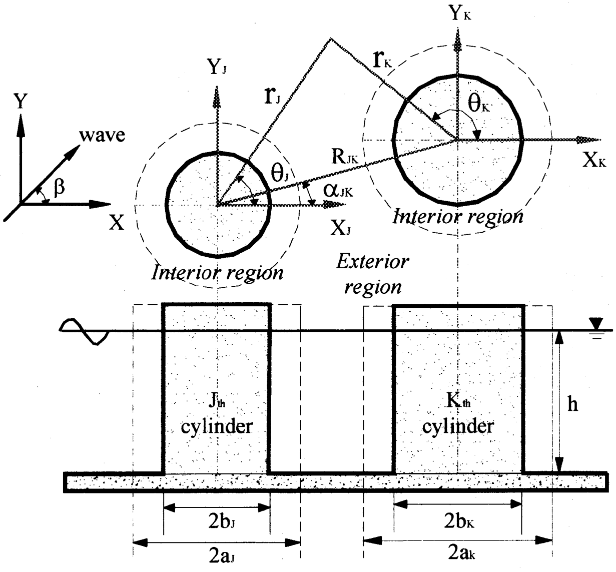

Fig. 1. Definition sketch of an array of dual cylinders

The array of the cylindrical structure is subjected to a train of regular waves of height H and angular frequency ω propagating at an angle β to the positive x-axis. For the uniform geometry of the array structure, the depth dependence of the problem can be factored out as follow:

$$\Phi(x,y,z,t) = R_e\left[\phi(x,y)f(z)e^{-i\omega t}\right] \tag{1}$$

in which, $Re[\,]$ denotes the real part of a complex expression and

$$f(z) = -\frac{ig(H/2)\cosh\kappa(z+h)}{\omega\cosh\kappa h} \tag{2}$$

in which g is the acceleration of gravity and the wave number k is the positive real root of the dispersion relation $\omega^2 = gk\tanh kh$.

The fluid domain is divided into $N+1$ regions: a single exterior region$(r>a_j)$ and N interior regions$(b_j<r<a_j)$. The velocity potential of incident wave with an angle β to the positive x-axis is presented in the jth local polar coordinate system as follow:

$$\phi_{in}^j = I_j e^{i\kappa r_j\cos(\theta_j-\beta)} \tag{3}$$

where $I_j\ (=e^{ik(x_j\cos\beta+y_j\sin\beta)})$ is a phase factor associated with cylinder j. Therefore, equation (3) can be represented as follow:

$$\phi_{in}^j = I_j\sum_{n\to-\infty}^{\infty} J_n(\kappa r_j)e^{in(\pi/2-\theta_j+\beta)} \tag{4}$$

in which J_n denotes the Bessel function of the first kind of order n. (Gradshteyn & Ryzhik (1965, p.973, equation M027)).

It can be shown that two-dimensional scattered velocity potentials from jth dual circular cylinder must satisfy a Helmholtz equation and the usual radiation boundary condition.

$$\left(\frac{\partial^2}{\partial r^2}+\frac{1}{r}\frac{\partial}{\partial r}+\frac{1}{r^2}\frac{\partial^2}{\partial\theta^2}+\kappa^2\right)\phi_s^j = 0 \tag{5}$$

$$(\kappa r)^{1/2}\left(\frac{\partial}{\partial r}-i\kappa\right)\phi_s^j \to 0 \quad as\ \ \kappa r\to\infty \tag{6}$$

On following boundary problems, the general form for the scattered wave emanating from cylinder j can be written as:

$$\phi_s^j = \sum_{n\to-\infty}^{\infty} A_n^j Z_n^j H_n(\kappa r_j)e^{in\theta_j} \tag{7}$$

in which, $Z_n^j\left(=Z_{-n}^j\right) = J_n'(\kappa a_j)/H_n'(\kappa a_j)$,

$$H_n(\kappa r_j) = J_n(\kappa r_j) + iY_n(\kappa r_j)$$

The total potential can thus be written as follow:

$$\begin{aligned}\phi_I &= \phi_{in} + \sum_{j=1}^{N}\phi_s^j \\ &= e^{ikr\cos(\theta-\beta)} + \sum_{j=1}^{N}\sum_{n=-\infty}^{\infty} A_n^j Z_n^j H_n(\kappa r_j)e^{in\theta_j}\end{aligned} \tag{8}$$

To take into account interactions among the cylindrical structures, it is necessary to evaluate the scattered potential ϕ_s^λ in terms of the representation of the incident potential ϕ_{in}^λ at structure j, $j=1,2,3,\ldots,N$, $j\neq\lambda$. This can be accomplished by using Graf's addition theorem for Bessel functions (Abramowitz and Stegun, 1972) to give,

$$H_n(\kappa r_\lambda)e^{in(\theta_\lambda-\alpha_{\lambda j})} = \sum_{m=-\infty}^{\infty} H_{n+m}(\kappa R_{\lambda j})J_m(\kappa r_j)e^{im(\pi-\alpha_{\lambda j}-\theta_j)} \tag{9}$$

in which, $j=1,2,3,\ldots,N$, $j\neq\lambda$. Equation (9) is valid for $r_j<R_{\lambda j}$, which is true on the boundary of the jth cylinder for all λ. The exterior region potential can be written as:

$$\begin{aligned}\phi_I = \sum_{n=-\infty}^{\infty}&\Bigg\{\Bigg[I_j e^{in(\pi/2-\beta)} \\ &+\sum_{\substack{\lambda=1\\ \lambda\neq j}}^{N}\sum_{m=-\infty}^{\infty} A_m^\lambda Z_m^\lambda H_{m-n}(\kappa R_{\lambda j})e^{i(m-n)\alpha_{\lambda j}}\Bigg]J_n(\kappa r_j) \\ &+ A_n^j Z_n^j H_n(\kappa r_j)\Bigg\}e^{in\theta_j}\end{aligned} \tag{10}$$

The potential in the jth interior region, ϕ_{II}^j, can be written as:

$$\phi_{II}^j = \sum_{n=-\infty}^{\infty} B_n^j\left[J_n(\kappa r_j) - \frac{J_n'(\kappa b_j)}{Y_n'(\kappa b_j)}Y_n(\kappa r_j)\right]e^{in\theta_j} \quad j=1,\ldots,N \tag{11}$$

where the B_n^j are unknown potential coefficients.

The boundary condition on the surface of cylinder j can be express as,

$$\frac{\partial\phi_I}{\partial r} = \frac{\partial\phi_{II}}{\partial r} \quad on\ \ r_j = a_j \quad j=1,2,\ldots,N \tag{12}$$

The wall of each cylinder is assumed to be thin with fine pores. The fluid flow passing through the porous wall is assumed to obey Darcy's law. Hence, the porous flow velocity is linearly proportional to the pressure difference across the thickness of the porous cylinder. Now the hydrodynamic pressure, $p(x,y,z,t) = Re(P(x,y)f(x)e^{-i\omega t})$, at any point in the fluid domain may be determined from the linearized Bernoulli equation as $p(x,y)= \rho i\omega\ \phi(x,y)$, where ρ is the fluid density. Therefore, it follows that

$$\frac{\partial \phi_{II}}{\partial r} = \frac{\gamma}{\mu}\rho i\omega\left[\phi_{II}^{j} - \phi_{I}\right] \quad on\ r_j = a_j \quad j = 1,2,...,N \quad (13)$$

in which μ is the coefficient of dynamic viscosity and γ is a material constant having the dimension of length. Subsequently, the porosity of the outer cylinder may be characterized by the dimensionless parameter $G=\rho\omega\gamma/(\mu k)$.

Finally, the diffracted component of the velocity potential in the exterior region must satisfy the usual radiation boundary condition as follow:

$$\lim_{r\to\infty}\sqrt{r}\left[\frac{\partial}{\partial r}(\phi_I - \phi_{in}) - i\kappa(\phi_I - \phi_{in})\right] = 0 \qquad (14)$$

where ϕ_{in} is the spatial component of the incident wave potential, given by $\phi_{in}=e^{ikr\cos(\theta-\beta)}$, where r is a global polar coordinate.

Applying boundary conditions, equation (10) and (11) lead to the following relationships between the potential coefficients A_n^j and B_n^j.

$$\begin{aligned} &I_j(i)^n e^{-in\beta} + \sum_{\substack{\lambda=1\\ \gamma\neq j}}^{N}\sum_{m=-\infty}^{m=\infty} A_m^\lambda Z_m^\lambda H_{m-n}(\kappa R_{\lambda j})e^{i(m-n)\alpha_{\lambda j}} \\ &= -\frac{s_n}{Y_n'(\kappa b_j)J_n'(\kappa a_j)}B_n^j - A_n^j \end{aligned} \qquad (15)$$

in which, $s_n = J_n'(\kappa b_j)Y_n'(\kappa a_j) - J_n'(\kappa a_j)Y_n'(\kappa b_j)$

$$\begin{aligned} &I_j(i)^n e^{-in\beta}J_n(\kappa a_j) + A_n^j Z_n^j H_n(\kappa a_j) \\ &+ \sum_{\substack{\lambda=1\\ \lambda\neq j}}^{N}\sum_{m=-\infty}^{m=\infty} A_m^\lambda Z_m^\lambda H_{m-n}(\kappa R_{\lambda j})e^{i(m-n)\alpha_{\lambda j}}J_n(\kappa a_{\lambda j}) \\ &= B_n^j\left[J_n(\kappa a_j) - \frac{J_n'(\kappa b_j)}{Y_n'(\kappa b_j)}Y_n(\kappa a_j)\right] \\ &+ \frac{i}{G}\left[J_n'(\kappa a_j) - \frac{J_n'(\kappa b_j)}{Y_n'(\kappa b_j)}Y_n'(\kappa a_j)\right] \quad j = 1,2,...,N \end{aligned} \qquad (16)$$

Combining equation (15) and (16), and using the Wronskian relationship for the Bessel functions, the following infinite systems of equations can be obtained by some calculations,

$$\begin{aligned} &A_n^j Z_n^j \Gamma_n^j + \sum_{\substack{\lambda=1\\ \lambda\neq j}}^{N}\sum_{m=-\infty}^{m=\infty} A_m^\lambda Z_m^\lambda H_{m-n}(\kappa R_{\lambda j})e^{i(m-n)\alpha_{\lambda j}} \\ &= -I_j(i)^n e^{-in\beta} \quad j = 1,2,...,N, -\infty < n < \infty \end{aligned} \qquad (17)$$

in which, $\Gamma_n^j = \dfrac{H_n'(\kappa a_j)s_n + \dfrac{2iG}{\pi\kappa a_j}H_n'(\kappa b_j)}{J_n'(\kappa a_j)s_n + \dfrac{2iG}{\pi\kappa a_j}J_n'(\kappa b_j)}$

$$B_n^j = \frac{Z_n^j \dfrac{2G}{\pi\kappa a_j}Y_n'(\kappa b_j)}{J_n'(\kappa a_j)s_n + \dfrac{2G}{\pi\kappa a_j}J_n'(\kappa b_j)}A_n^j \qquad (18)$$

In order to calculate the potential coefficients A_n^j, the infinite system in equation (17) is truncated to a $(2M+1)N$ system of equations with $(2M+1)N$ unknowns,

$$\begin{aligned} &I_j(i)^n e^{-in\beta} + \sum_{\substack{\lambda=1\\ \lambda\neq j}}^{N}\sum_{m=-M}^{m=M} A_m^\lambda Z_m^\lambda H_{m-n}(\kappa R_{\lambda j})e^{i(m-n)\alpha_{\lambda j}} \\ &= -A_n^j Z_n^j \Gamma_n^j \quad j = 1,2,...,N, -\infty < n < \infty \end{aligned} \qquad (19)$$

Good accuracy can be achieved by increasing M in spite of the expense of computing time. Except for the cylinders being very close together, taking $M=10$ could produce accurate results to all examinations. The potential coefficients B_n^j may then be obtained from equation (18). The velocity potentials in each fluid region may be determined in the same manner.

For example, taking $N = 1$ in equation (17) and assuming that the cylinder center is located at the origin for $\beta=0$, it can be expressed with,

$$\begin{aligned} A_n^1 &= -(i)^n \frac{J_n'(\kappa a_1)s_n + \dfrac{2iG}{\pi\kappa a_1}J_n'(\kappa b_1)}{Z_n^1\left[H_n'(\kappa a_1)s_n + \dfrac{2iG}{\pi\kappa a_1}H_n'(\kappa b_1)\right]} \\ B_n^1 &= -(i)^n \frac{\dfrac{2iG}{\pi\kappa a_1}Y_n'(\kappa b_1)}{H_n'(\kappa a_1)s_n + \dfrac{2iG}{\pi\kappa a_j}H_n'(\kappa b_1)} \end{aligned} \qquad (20)$$

Equation (20) represents the limiting case of wave interaction with an inner cylinder reported by Wang and Ren (1994).

The wave force on the jth outer cylinder is also determined by integrating the pressure over the surface of the cylinder as follow:

$$\begin{aligned} F_{ex}^j &= -\frac{\rho g(H/2)a_j}{\kappa}\tanh\kappa h \\ &\times \int_0^{2\pi}\left[\phi_I(a_j,\theta_j) - \phi_{II}(a_j,\theta_j)\right]\begin{Bmatrix}\cos\theta_j\\ \sin\theta_j\end{Bmatrix}d\theta_j \end{aligned} \qquad (21)$$

in which the upper element of a bracketed pair refers to the force in the x-direction and the lower element to that in the y-direction. Performing the integration, the wave force subjected to the jth outer cylinder can be expressed with,

$$\begin{aligned} F_{ex}^j &= -\begin{Bmatrix}i\\ 1\end{Bmatrix}\frac{\rho g H\tanh\kappa h}{\kappa^2 H_1'(\kappa a_j)} \\ &\times \frac{J_1'(\kappa a_j)s_1}{J_n'(\kappa a_j)s_1 + \dfrac{2iG}{\pi\kappa a_j}J_n'(\kappa b_j)}\left(A_{-1}^j\begin{Bmatrix}-\\ +\end{Bmatrix}A_1^j\right) \end{aligned} \qquad (22)$$

The wave force on the jth inner cylinder can also be expressed with,

$$F_{In}^{j} = -\begin{Bmatrix} i \\ 1 \end{Bmatrix} \frac{\rho g H \tanh \kappa h}{\kappa^2 Y_1'(\kappa b_j)} \left(B_{-1}^{j} \begin{Bmatrix} - \\ + \end{Bmatrix} B_1^{j} \right) \tag{23}$$

Moreover, the wave run up of the jth cylinder is calculated as follow:

$$\eta^{(O)}(a_j, \theta_j) = \frac{H}{2} \sum_{n=-M}^{M} A_n^j Z_n^j \left[H_n(\kappa a_j) - \Gamma_n^j J_n(\kappa a_j) \right] e^{in\theta_j} \tag{24}$$

$$\eta^{(I)}(a_j, \theta_j) = \frac{H}{2} \sum_{n=-M}^{M} B_n^j \left[J_n(\kappa a_j) - \frac{J_n'(\kappa b_j)}{Y_n'(\kappa b_j)} Y_n(\kappa a_j) \right] e^{in\theta_j} \tag{25}$$

$$\eta^{(O)}(b_j, \theta_j) = \frac{H}{2} \sum_{n=-M}^{M} \left[\frac{2B_n^j}{\pi \kappa b_j Y_n'(\kappa b_j)} \right] e^{in\theta_j} \tag{26}$$

in which, $\eta^{(O)}(a_j, \theta_j)$, $\eta^{(I)}(a_j, \theta_j)$ and $\eta^{(O)}(b_j, \theta_j)$ denote the wave run up on exterior surface of the outer cylinder, on interior surface of the outer cylinder and exterior surface of the inner cylinder, respectively.

2.2 Dynamic response due to wave forces

The dynamic response of an offshore structure due to wave force is significantly depended on the wave force evaluation. It is known that the diffraction theory is more suitable for the wave force evaluation of structure with relatively large diameter. Otherwise, the wave force evaluation of many offshore structures is performed with the Morison equation. If the inertia term on the wave force leads to the dominant effects on the wave force evaluation, it can be implemented with the Morison equation of which the coefficient is modified with the diffraction result. The wave force can be evaluated with the water particle motion such as velocity and acceleration. For an idealized dual cylindrical structure as shown in Fig.2, the governing equation of motion can be expressed with the finite element method as follow:

$$[M]\{\ddot{x}\} + [C]\{\dot{x}\} + [K]\{x\} = \{F\} \tag{27}$$

in which $[M]$, $[C]$ and $[K]$ denote the mass matrix, damping matrix, and stiffness matrix, respectively, and $\{x\}$ denotes the displacement vector. Using the Morison equation, the external wave force $\{F\}$ can be expressed with the inertia force and drag force.

$$\{F\} = [\overline{C}_M]\{\ddot{v}\} - [\overline{C}_m]\{\ddot{x}\} + [\overline{C}_D]\{(\dot{v} - \dot{x})|\dot{v} - \dot{x}|\} \tag{28}$$

in which

$$\begin{aligned} [\overline{C}_M] &= [\ddots \rho C_M V \ddots] \\ [\overline{C}_m] &= [\ddots \rho (C_M - 1) V \ddots] \\ [\overline{C}_D] &= \left[\ddots \rho C_D \frac{A}{2} \ddots\right] \end{aligned} \tag{29}$$

where $\{\dot{v}\}$ and $\{\ddot{v}\}$ denote the velocity and acceleration of the water particle and the inertia coefficient (C_M) and the drag coefficient(C_D) is 2 and 1, respectively. For the structure subjected to the diffraction and the wave force interaction, the wave force can be evaluated with the acceleration of water particle. Obtaining the acceleration of the water particle, the wave force on the structure can be determined with the equivalent nodal force expressed with the shape function.

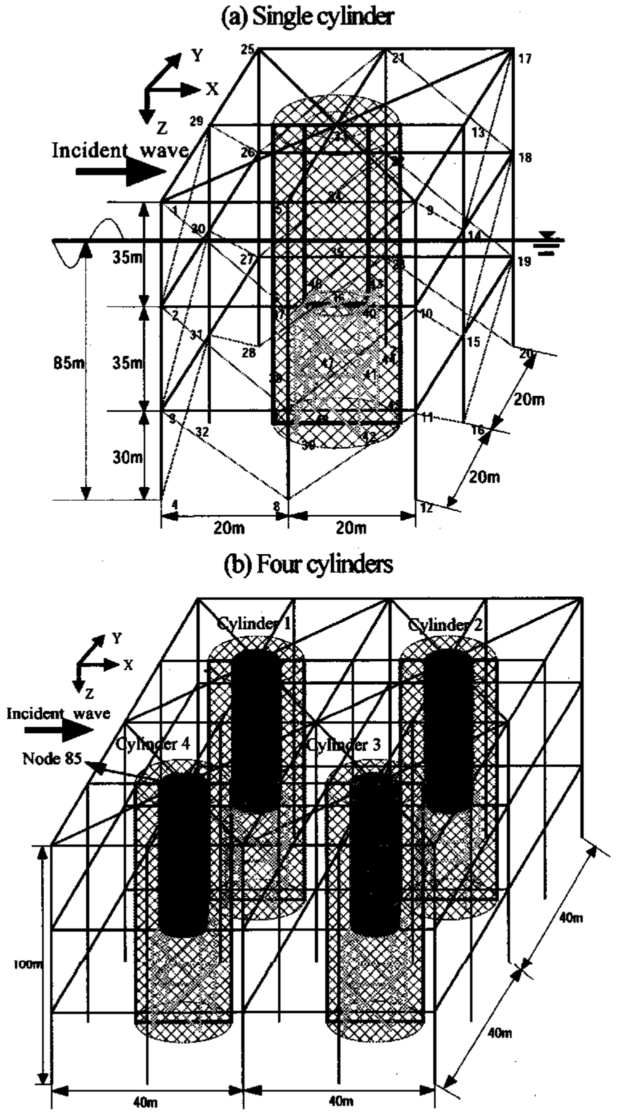

Fig.2 Analytical model of dual cylindrical structure.

To apply the wave force interaction to the inertia force in Morison equation, the acceleration($\ddot{v}$) can be alternated with $\ddot{v}_M$ as follow:

$$F_{In}^{j} = C_M \rho \frac{\pi D^2}{4} \ddot{v}_M \tag{30}$$

Using equation (23), the water particle acceleration on the wave force interaction can be expressed with,

$$\ddot{v}_M = \frac{-i\rho g H}{\kappa} \frac{\cosh \kappa s}{\cosh \kappa d} \frac{1}{Y_1'(\kappa b_j)} \left(B_{-1}^j - B_1^j\right) \cos(\omega t - \alpha) \frac{1}{C_M \rho \pi a^2} \tag{31}$$

If the dynamic response is restrained within linear response, the governing equation of motion can be expressed with equation (31),

$$\left[\tilde{M}\right]\{\ddot{x}\}+\left[\tilde{C}\right]\{\dot{x}\}+[K]\{x\}=\left[\bar{C}_M\right]\{\ddot{v}_M\} \tag{32}$$

in which

$$\begin{aligned}\left[\tilde{M}\right]&=\left[[M]+\left[\bar{C}_m\right]\right],\\ \left[\tilde{C}\right]&=\left[[C]+\left[\bar{C}_D\right]\right]\end{aligned} \tag{33}$$

Applying the eigenvalue analysis for equation (32), it can be expressed with the following equation.

$$[I]\{\ddot{q}\}+\left[\ddots\left(2\beta_j\omega_j+\tilde{C}_D\right)\ddots\right]\{\dot{q}\}+\left[\ddots\omega_j^2\ddots\right]\{q\}=\{\tilde{f}\} \tag{34}$$

in which

$$\begin{aligned}&\{x\}=[\Phi]\{q\},\ [I]=[\Phi]^T\left[\tilde{M}\right][\Phi]\\ &\left[\ddots\left(2\beta_j\omega_j+\tilde{C}_D\right)\ddots\right]=[\Phi]^T\left[\tilde{C}\right][\Phi]\\ &\left[\ddots\omega_j^2\ddots\right]=[\Phi]^T[K][\Phi]\\ &\{\tilde{f}\}=[\Phi]^T\{\tilde{F}\}\end{aligned} \tag{35}$$

Equation (34) can be solved by step-by-step integration such as Newmark β method.

3. Numerical results and discussions

3.1 Wave interaction to dual cylindrical structure

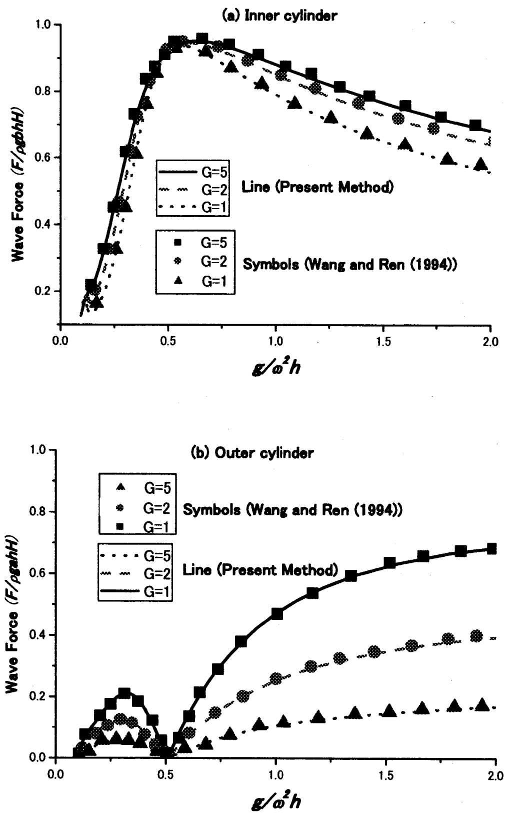

Fig.3 Comparison of dimensionless wave forces on a concentric porous cylinder for $b/a=1/2, \beta=0$.

In order to examine the validity of the wave force evaluation, the comparisons are made by the results from Wang & Ren(1994). Fig. 3 shows the comparison of wave forces on a concentric porous cylinder. The various parameters are $b/a=0.5$, $G=1,\ 2,\ 5$ and $\beta=0$, respectively. The abscissa denotes the nondimensional frequency, g/ω^2h, and the vertical axis is the nondimensionalized wave force normalized with $\rho gahH$ and $\rho gbhH$. The wave force on inner cylinder is gradually increased and the wave force on outer cylinder is significantly decreased as the porosity(G) becomes a large one. It is noted that the wave force on inner cylinder is increased by the wave infiltration which percolates in the inside as increased the porosity of outer cylinder. It is shown that the present method gives the good agreement to the results from Wang & Ren(1994). Therefore, the present method is very available to evaluate the wave forces on the dual cylindrical structure.

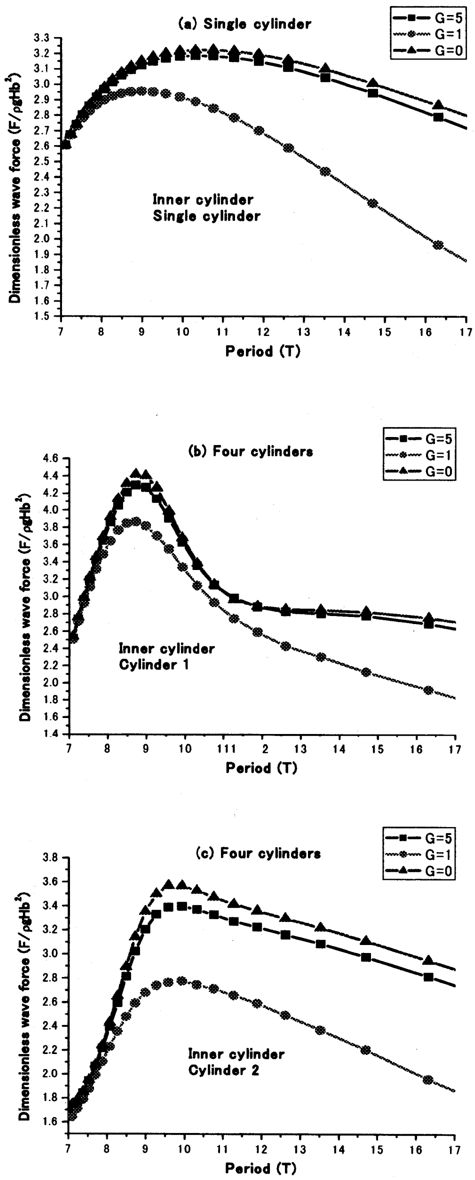

Fig.4 Comparison of dimensionless wave forces on dual cylinders for $b/a=2/3, \beta=0$.

It is examined about the effects due to the porosity of outer cylinder and the number of dual cylinders for the wave force evaluation. Dimensionless wave forces on dual cylinders are shown in Fig. 4. The various parameters are $b/a=2/3$, $h=85m$ and $\beta=0$, respectively. The radius of inner cylinder is installed $10m$ for all cases. Four cylinders are numbered clockwise 1-4 and are situated at (-20,20), (20,20), (20,-20), and (-20,-20), respectively. Since the wave forces of cylinder 1 and 4, 2 and 3 have the same values, the wave forces of cylinder 3 and 4 are not demonstrated in Fig. 4. The wave force on inner cylinder for all cases is gradually increased as the porosity(G) of outer cylinder becomes a large one. When the porosity(G) of outer cylinder is 5, the wave force on inner cylinder is similar to the values of $G=0$. It is known that it corresponds to the wave force acting on only inner cylinder without outer cylinder. Finally, if the porosity of outer cylinder becomes a large one, the effects of outer cylinder do not contribute to the wave force of inner cylinder. Comparing the single cylinder with the four cylinders, the wave forces of four cylinders are generally larger than that of single. It is understood that interaction between the wave and structures leads to considerable influences on the wave force of the dual cylindrical structure with the porosity. For four cylinders, the wave force of cylinder 1 is larger than the cylinder 2 as the wave period is decreased. The interaction plays important roles on the wave force evaluation for the dual cylindrical structure. It is also understood that the interaction effects are closely related to the wave period and the number of dual cylinders.

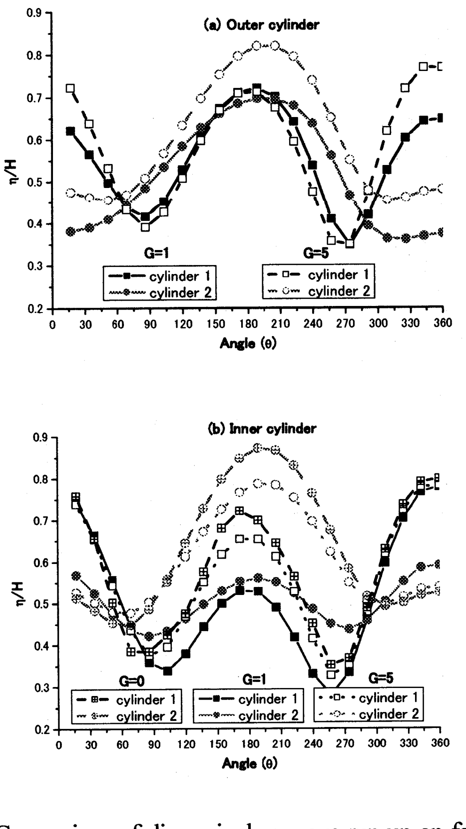

Fig.5 Comparison of dimensionless wave run up on four dual cylinders for $b/a=2/3$, $T=9sec$ and $\beta=0$.

Dimensionless wave run up on four cylinders is shown in Fig. 5. It is noticed that the wave run up of outer cylinder and inner cylinder is gradually magnified by increasing the porosity(G). The wave run up of outer cylinder for $G=5$ is larger than $G=1$ because the reflection from inner cylinder considerably affects the outer cylinder. The wave run up of inner cylinder is inversely decreased by the effects of outer cylinder. There is relatively considerable difference for wave run up of cylinder 1 and 2 by the effects of interaction. It is understood that the wave run up for dual cylindrical structure is closely related to the porosity(G) of outer cylinder and the effects of interaction.

3.2 Dynamic responses of dual cylindrical structure

The dynamic response is examined by using the wave force evaluation as influenced by the porosity(G) of outer cylinder and the number of dual cylinders. The structure properties of dual cylindrical structure are shown in Fig. 2. The single cylinder of dual cylindrical structure consists of three segments. The one is a large size impermeable cylinder($D=20m$) which is surrounded with permeable outer cylinder($D=30m$), the second is a middle size pipe($D=2m$) which can support the weight of a large size impermeable cylinder and the other segment is a small size pipe($D=1m$) of which the outside frame of structure is built. The structure has the properties that unit weight is $77.0(kN/m^3)$, Yong modulus $210GPa$ and shear stiffness coefficient $81GPa$. The nodal points 1, 5, 9, 13, 17, 21, 25 and 29 are added the load of $1MN$, respectively. And the top of a large impermeable cylinder is added the load of $35MN$. The four cylindrical structure is composed of the single cylindrical structure that has the same properties.

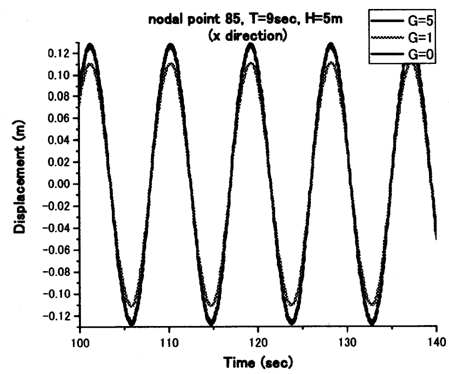

Fig.6 Time histories of displacement responses for four cylinders.

Fig. 6 shows the time histories of displacement responses at the nodal point 85 for the wave height, $5m$ and the wave period, $9sec$. The nodal point 85 is located on the top of the cylinder 4 of four cylinders. Wave period is chosen at $9sec$ because it yields the largest wave force acting on structure to relevant region of wave period. The displacement responses of $G=5$ and $G=0$ are very similar ones because the wave force on structure have a similar one as shown in Fig. 4. The difference between $G=5$ and $G=1$ of four cylinders turns out larger than the single cylinder because the interaction effects between the wave and structures are caused by increasing the number of dual cylinders. It is noticed that the porosity(G) of outer cylinder and the number of dual cylinders lead to important effects on the displacement response.

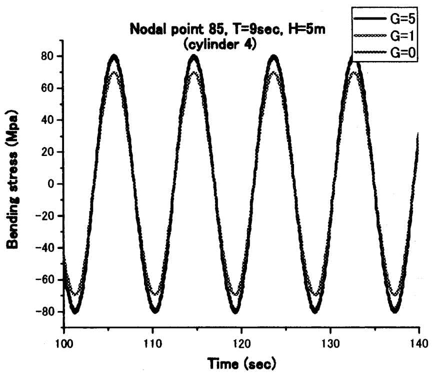

Fig.7 Time histories of bending stress responses for four cylinders.

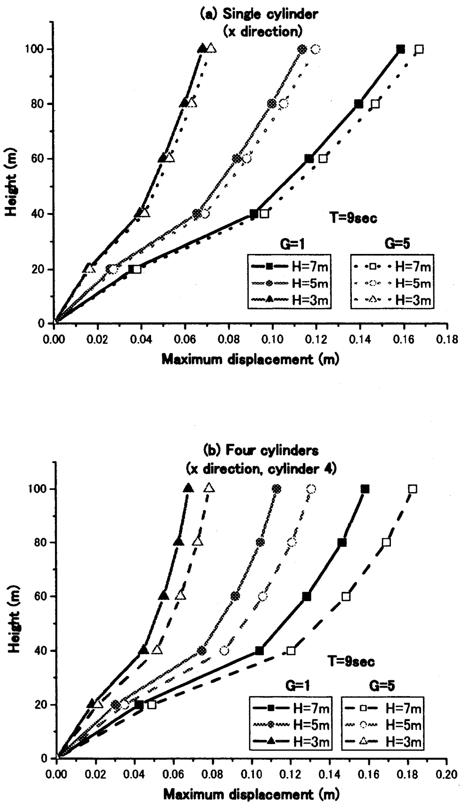

Fig.8 Relation between maximum displacement responses and wave height.

Fig. 7 also shows the time histories of the bending stress at the nodal point 85. The response of bending stress becomes the same tendency as the displacement response. The response of four cylinders is influenced by the moment that is caused by the differences of wave forces between the cylinder 1 and 2 as shown in Fig. 4. From these results, it is understood that the interaction between the wave and structures plays important roles on the dynamic response of the dual cylindrical structure.

Fig. 8 shows the relation between maximum displacement response and wave height. Because the response of $G=0$ is very similar to one of $G=5$, it is not represented in the figure. The three lines correspond to the wave height from *3m* to *7m* and the wave period, *9sec*, respectively. By comparing the responses between $G=1$ and $G=5$, the difference is increased by the increment of the wave height. While the displacement responses between the four dual cylindrical structure and the single dual cylindrical structure become relatively similar ones for $G=1$ and $G=5$, the difference is enlarged for increasing the wave height. Since the rigidity of the framed structure composed of the deck is considerably larger than the one of the column structure set up the side of the cylinder structure, it is supposed to increase the interaction effects on the wave force and the structure for the four cylinder structure.

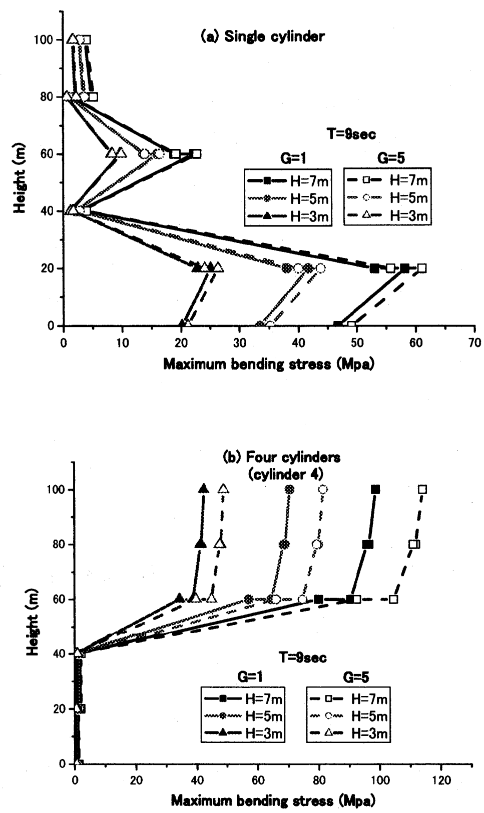

Fig.9 Relation between maximum bending stress responses and wave height.

Fig. 9 shows the relation between responses of maximum bending stress and wave height. The difference between $G=1$ and $G=5$ also has a similar tendency on the displacement response for increasing the wave height. It is understood that the maximum bending stress of the single cylinder structure turns out considerably different results to the four cylinder structure. It is suggested that since the framed structure is constructed by very rigid member, the four cylinder structure is subjected to the combined force at the top of cylinder by the rigid structure. Thus, the bending stress of the four cylinders increases at the top of the cylinder and inversely reduces at the bottom of the structure. It is understood that the bending stress is considerably affected by the moment caused by the difference of wave forces between the cylinder 1 and 2. It is very effective for the four cylinder structure to reduce the bending stress of the frame structure under the impermeable cylinder. It is suggested that the combined structure such as the four dual cylindrical structure has the dynamic characteristics to enhance the safety by reducing the bending stress of the frame structure.

Fig. 10 shows the relation between the maximum displacement response and wave height. Fig. 11 also shows the relation between the maximum bending stress and wave height. Comparing the responses for $G=1$ and $G=5$, there is considerable difference for all wave periods. It is understood that the evaluation of interaction between the wave and structures plays important roles on dynamic responses for the four dual cylindrical structure. For developing the large scale offshore platform, it is supposed to be very effective to apply the dual cylindrical structure with the appropriate porosity of outer cylinders and the number of dual cylinders.

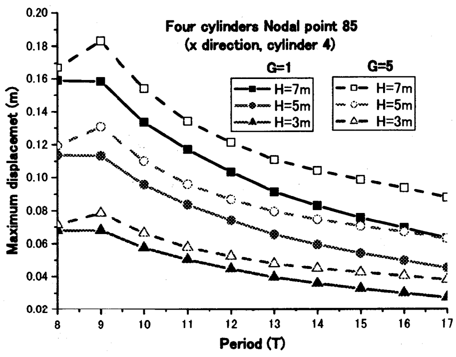

Fig.10 Relation between maximum displacement responses and wave height for four cylinders.

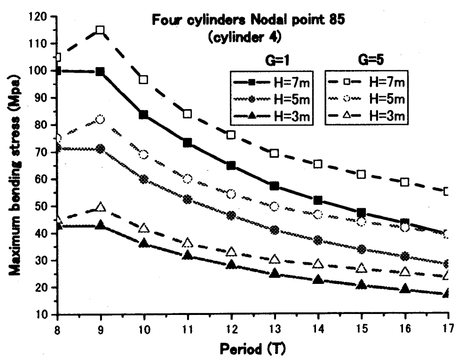

Fig.11 Relation between maximum bending stress responses and wave height for four cylinders.

4. Conclusion

The dynamic response characteristics of dual cylindrical structure are examined. The results are summarized as follows:

(1) It is shown that the analytical method for wave force evaluation is very useful to evaluate the wave forces on dual cylindrical structure with the interaction.

(2) It is suggested that if the appropriate porosity can be provided into the outer cylindrical structures, the dynamic response due to wave force could be effectively reduced by the dual cylindrical structure.

(3) Since the present method can be effectively applied to evaluate the interaction effects between the wave and structures, the dynamic response evaluation can be carried out for the dual cylindrical structure which has great possibilities of developing the large scale offshore structure.

References

1) Chakrabarti S. K., *Hydrodynamics of offshore structure*, Computational mechanics publications, 1987

2) Kawano, K.. and Venkatarama K. and Hashimoto, H., Seismic response effects on large offshore platform, *Proc. Of the Ninth Inter. Offshore and polar engineering conference.* VolVI, pp.528-535, 1990

3) Kawano, K. and Komasa, K. and Miyazaki, Y. and Hashimoto, H., Dynamic response analyses of offshore platform with buoyancy type large members, *Proc, Of the Sixth Inter. Offshore and polar eng. Conf.* Vol1, pp.176-181, 1996

4) Kawano, K. and Venkatartamana, K. and Hashimoto, T., Nonlinear dynamic responses of a large offshore structure due to wave forces, *Proc. Of the ICASP8 conference,. Appl. Of statistics and probability*, pp.781-797, 1999

5) Linton. C. M. and Evans. D. V., The interaction of waves with arrays of vertical circular cylinder, *J. Fluid Mechl.* 215, pp. 549-569, 1990

6) MacCamy, R.C. and Fuchs, R.A., *Wave forces on piles: a diffraction theory*, Tech. Memo No. 69, US Army Corps of Engineers, Beach Erosion Board, 1954

7) Sankarbabu, K. and Sannasiraj, S.A. and Sundar, V., Interaction of regular waves with a group of dual porous circular cylinders, *Applied Ocenan Research*, Vol. 29, No. 4, pp 180-190, 2007

8) Spring, B. H. and Monkmeyer, P. L., Interaction of plane waves with vertical cylinders, *In Proc. 14th Intl Conf. on Coastal Engineering, Chap. 107*, pp. 1828-1845, 1974

9) Wang, K.H. and Ren, X., Wave interaction with a concentric porous cylinder system, *Ocean Engineering*, Vol. 21, pp 343-360, 1994

(Received: April 14, 2008)